Available online at www.sciencedirect.com
ScienceDirect
Journal of Petroleum Science and Engineering 59 (2007) 219–225
JOURNAL OF PETROLEUM SCIENCE & ENGINEERING
www.elsevier.com/locate/petrol

High-temperature hydrogen sulfide corrosion on the heat-affected zone of the AISI 444 stainless steel caused by Venezuelan heavy petroleum

Cleiton C. Silva [a], João Paulo S.E. Machado [a], Ana V.C. Sobral-Santiago [c], Hosiberto B. de Sant'Ana [b,*], Jesualdo P. Farias [a]

[a] *Universidade Federal do Ceará, Department of Materials and Metallurgical Engineering, Campus do Pici, Building 715, Welding Engineering Laboratory, CEP: 60455-760, Fortaleza, Ceará, Brazil*
[b] *Universidade Federal do Ceará, Department of Chemical Engineering, Campus do Pici, Building 709, Fuel and Lubricants Laboratory, CEP: 60455-760, Fortaleza, Ceará, Brazil*
[c] *Faculdade Christus, Av. Dom Luiz, 911, CEP: 60160-230, Meireles, Fortaleza, Ceará, Brazil*

Received 4 March 2005; received in revised form 16 April 2007; accepted 19 April 2007

Abstract

The aim of this study was to evaluate the effect of welding on the corrosion resistance of the heat-affected zone (HAZ) of the AISI 444 ferritic stainless steel in medium containing Venezuelan heavy oil. AISI 444 steel plates were welded through the use of three levels of welding heat input (4, 6 and 8 kJ/cm). Samples were extracted from the welded plates and thermally treated in three different temperatures (200, 300 e 400 °C), while immerged in petroleum for a period of 4 h. Optical microscopy (OM), scanning electronic microscopy (SEM) and energy dispersive X-ray analysis (EDX) techniques were used for the analysis of the surface and transversal section of the joint. Electrochemical trials of cyclic potentiokinetic reactivation of double loop (EPR-DL) were also carried out. It has been concluded that the temperature of treatment has direct influence on the level of material corrosion and that the increase in the welding heat input contributes to a higher level of corrosion.

Keywords: AISI 444 stainless steel; Heat-affected zone; Corrosion resistance

1. Introduction

Its perfect match between mechanical properties and resistance to corrosion justifies the increasing use of stainless steel in the industrial sector. These types of steel are divided in five main groups according to its metallurgical characteristics (Folkhard, 1988). Among the various stainless steels types, we highlight the AISI 444 ferritic stainless steel, which presents a thoroughly ferritic microstructure and whose chemical composition is differentiated by a reduction in the concentration of interstitials elements, as carbon and nitrogen, and addition of molybdenum in order to improve its corrosion resistance, and addition of stabilizing elements such as titanium and niobium (Sedricks, 1996).

* Corresponding author. Tel.: 55 85 3366 9611/9594; fax: 55 85 3366 9611.
E-mail addresses: cleitonufc@yahoo.com.br (C.C. Silva), jpufcmec@bol.com.br (J.P.S.E. Machado), avladia@secrel.com.br (A.V.C. Sobral-Santiago), hbs@ufc.br (H.B. de Sant'Ana), jpf@secrel.com.br (J.P. Farias).

0920-4105/$ - see front matter © 2007 Elsevier B.V. All rights reserved.
doi:10.1016/j.petrol.2007.04.003

Table 1
Physical–chemical analysis of the crude oil used

Specific gravity °API	Pour point (°C)	Viscosity at 50.0 °C (cSt)	Sulfur content (% m/m)
12.2	0	1500	4

The welding processes are frequently used in the manufacturing and repairing of equipment and components made of stainless steel. Regarding the ferritic stainless steel, the thermal cycle produced during the welding may be enough to cause phase precipitation in the heat-affected zone (HAZ). Many times the presence of these phases is associated with ductility and toughness reduction and the increase in hardness, by causing material embrittlement (Grobner, 1973; Cortie and Pollak, 1995; Silva et al., 2007). Corrosion resistance can also be altered mainly when phenomenon such as sensitization is likely to occur (Sedricks, 1996; Silva et al., 2007). Besides that, these types of steel may more frequently present problems related to corrosion when applied to equipment that processes crude oil for the fact that they operate in temperatures ranging from 200 to 500 °C.

One of the most important equipment found in a unit of petroleum processing is the distillation tower, which changes crude oil into various fractions. These towers have an internal coating of AISI 405 stainless steel in order to resist the attack of corrosive substances deriving from the processing of petroleum. However, the high acidity level in heavy petroleum leads to the degradation of this coating (Cosultchi et al., 2001; Turnbull and Griffiths, 2003). The most common repairing technique uses AISI 316L austenitic stainless steel lining, carrying out the SMAW process. But this material has presented problems with corrosion, when under tension, associated to thermal fatigue (Cayard et al., 1994; Sedricks, 1996). One alternative to recover the worn out distillation towers in study in the Federal University of Ceará is to apply AISI 444 ferritic stainless steel lining as a substitute for the AISI 316L stainless steel (Machado et al., 2006; Silva et al., 2006, submitted for publication). The present work aims to study the alterations in the metallurgic characteristics in the heat-affected zone of the AISI 444 ferritic stainless steel and its influence on the resistance to corrosion of the heat-affected zone (ZAC) in medium containing Venezuelan heavy petroleum of the "Bacha-queiro" type.

Table 2
Chemical composition of the stainless steel AISI 444 (% weight)

C	Mn	Si	P	S	Cr	Ni	Mo
0.015	0.121	0.54	0.024	0.001	17.558	0.201	1.857
Al	Cu	Co	V	Nb	Ti	N	O
0.011	0.0343	0.017	0.045	0.162	0.129	0.123	0.023

Table 3
Chemical composition of the welding metal of the electrode AWS E309MoL-16—analysis by the furnisher (% weight)

C	Cr	Ni	Mo
0.03	23	13	2.5

2. Experimental procedure

The crude oil used in this study was provided by Refinaria Lubrificantes Nordeste LUBNOR/PETROBRAS without previous processing. The following properties were determined: density, fluidity point, viscosity and sulfur concentration. The results of these analysis are shown in Table 1.

The AISI 444 ferritic stainless steel, whose chemical composition is shown in Table 2, was used as base metal. The AWS E 309MoL-16 austenitic stainless covered electrode was used as filler metal. The chemical composition of the filler metal, according to the manufacturer, is shown in Table 3.

The bead on plate welding in the plane position was made on AISI 444 steel sheet, which had 50×150 mm dimension and 3.15 mm thickness, using the shielding metal arc welding (SMAW) process. The procedure was carried out manually with the help of a guide machine for the control of the welding speed. An INVERSAL 450 multiprocess welding source and a data acquisition system were used. Three levels of welding energy (4, 6 and 8 kJ/cm), whose parameters are shown in Table 4, were used in this work.

After the welding the sheets went through a process of cleaning for the removal of slag. The sheets were cut into samples of 12×25×3.15 mm, comprising part of the welding metal, the heat-affected zone and the base metal. The samples were submitted to thermal treatments at three levels of temperature, 200, 300 and 400 °C and immersed in heavy oil for 4 h, aiming at reproducing the

Table 4
Used welding parameters (in CC $^{+}$)

Rms current (A)	Rms voltage (V)	Welding speed (cm/min)	Electrode diameter (mm)	Welding energy (kJ/cm)
102	24.6	35	4.0	4.2
102	25.4	25	4.0	6.2
103	26.4	20	4.0	8.1

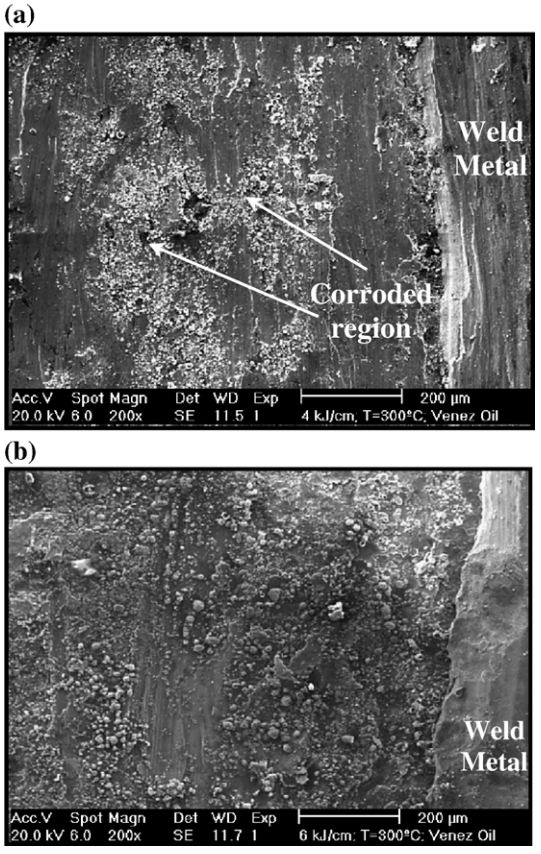

Fig. 1. SEM of the HAZ region near the weld bead, both treated with petroleum at 300 °C. (a) Sample welded with 4 kJ/cm. (b) Sample welded with 6 kJ/cm (200×).

severe working conditions of the stainless steel in operation in the distillation towers, where they are in direct contact with the heated petroleum. It should be noticed that two samples at each welding heat input were treated at each temperature levels tested in this work. The thermal treatments were carried out at the lubricant and fuel laboratory (LCL) of the Federal University of Ceará, using a flash point apparatus.

After the heat treatment, the samples were cleaned with toluene and n-pentane for further evaluation of the surface, which was carried out through the scanning electronic microscopy (SEM) and energy dispersive X-ray analysis (EDX), to evaluate the kind of corrosion present and the influence of heavy oil in the samples. Samples were conventionally prepared for the metallographic analysis of the transversal section of the test specimen. The samples were analyzed through optical microscopy (OM), scanning electronic microscopy (SEM) and energy dispersive X-ray analysis (EDX).

An image analyzer was used to evaluate the grain size of the heat-affected zone. The cyclic potentiokinetic reactivation of double loop (EPR-DL) technique was used to check the occurrence of sensitization phenomenon in the heat-affected zone, which is based on the stability of a passive state that, for the stainless steel, depends on the chromium contained in the solid solution, therefore detecting the main cause for the intergranular corrosion, which is the chromium depletion of the matrix, which occurs through the complex chromium carbides precipitation (Lundin et al., 1986; Folkhard, 1988; Sedricks, 1996). The result of this trial is shown in the form of two curves plotted on a graph. One of the curves refers to the anodic polarization and the other to the reverse polarization. The peaks of each curve correspond to the maximum values of the current (I) reached. The ratio I_r/I_a is used to measure the level of sensitization (Luz et al., 2006). According to Majidi and Streicher (1986), current rates (I_r/I_a) with values lower than 0.001 correspond to the step structure, that is, one free from precipitation. Rates ranging from 0.001 and 0.05 indicate a dual structure, where some of the precipitates are observed, but which do

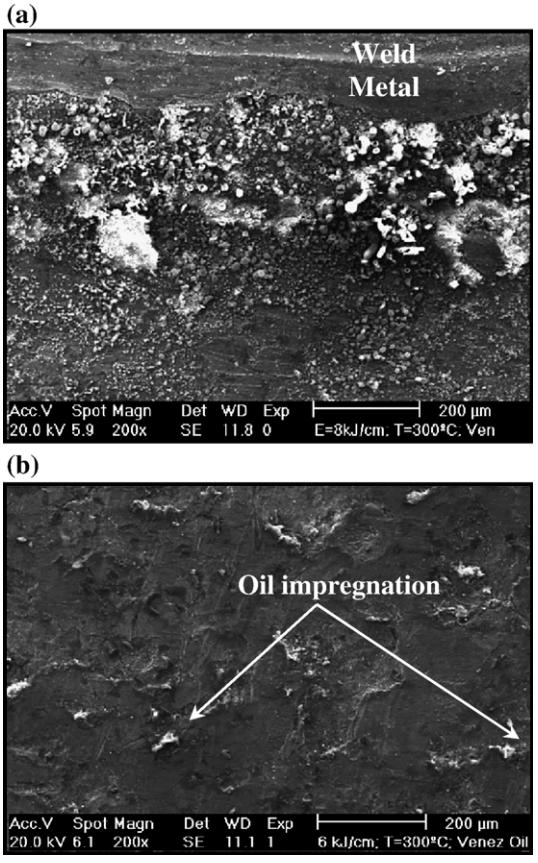

Fig. 2. Scanning electronic microscopy (a) Sample welded with 8 kJ/cm treated with petroleum at 300 °C. (b) Base metal of the samples welded with 6 kJ/cm at 300 °C. It should be noted that the absence of corroded regions. The clear area are impregnated with oil (200×).

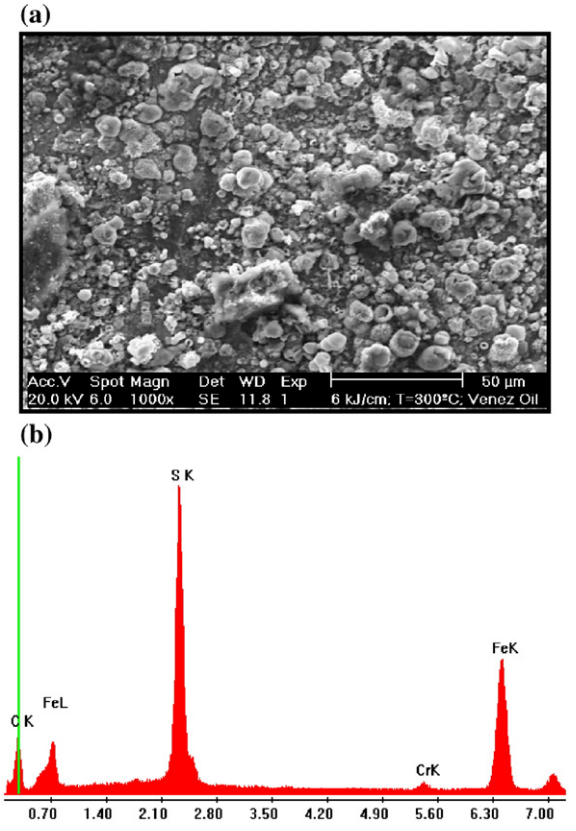

Fig. 3. Scanning electronic microscopy (a) Sample welded with 6 kJ/cm and treated with petroleum at 300 °C. Sulfide iron grains nucleation (FeS) (200×). (b) EDX analysis of the region showed in panel a.

not completely surround the grain. Rates higher than 0.05 correspond to a ditch structure, with grains completely surrounded by chromium carbides. However, this relation applies to materials whose ASTM grain size is around 3.5. The trials were carried out in the heat-affected zone (HAZ) within an area of 1.5 mm starting from the limit of the partially melted zone (PMZ). In this area there is a higher probability of chromium carbides precipitation for the ferritic stainless steel, since the temperatures rise above 900 °C.

3. Results and discussion

3.1. Superficial analysis

The superficial analysis revealed an intense attack on the HAZ adjoining the weld bead. Areas in corrosion process caused by the activity of corrosive substances deriving from phase transformation and chemical reactions of petroleum were observed. In the samples welded with the lowest heat input (4 kJ/cm), some areas in corrosion process were observed for the samples treated at 200 °C and 300 °C (Fig. 1a). Corrosion was stronger at the temperature of 400 °C and basically the whole area surrounding the weld bead was attacked.

The sample welded with heat input of 6 kJ/cm and treated at 200 °C presented local corrosion, similar to the aspect shown in Fig. 1a, although when treated at 300 °C and 400 °C the superficial analysis indicated an intense process of corrosion, as shown in Fig. 1b. The samples welded with heat input of 8 kJ/cm presented severe corrosion in the heat-affected zone in all temperatures of treatment (Fig. 2a). Fig. 2b shows the surface of the base metal of the sample welded with 6 kJ/cm and treated at 300 °C, where no corroded area was observed.

After a detailed analysis of the corroded areas in the samples, it was possible to observe nucleated particles on the surface with granular morphology (Fig. 3a). The chemical composition of the particles presented in Fig. 3b, and obtained through the EDX analysis, shows high quantities of sulfur and iron, besides the presence of carbon and chromium. This observation is important since it shows that the process of corrosion occurred due to the high concentration of sulfur present in the Venezuelan petroleum, resulting in the formation of iron sulfide as the corrosion product.

This corrosion type is characteristic of equipment in the petroleum industries, which produce and refine petroleum. Medvedeva (2000) classify this corrosion type as high-temperature hydrogen-sulfide corrosion (HTHC). The HTHC generally occurs under the influence of hydrogen sulfide (H_2S), which may be present in operations where petroleum is processed with high concentrations of sulfur. When heated at temperatures higher than 260 °C this kind of oil promotes the decomposition of sulfurated compounds and the formation of H_2S (Medvedeva, 2000). The process of corrosion

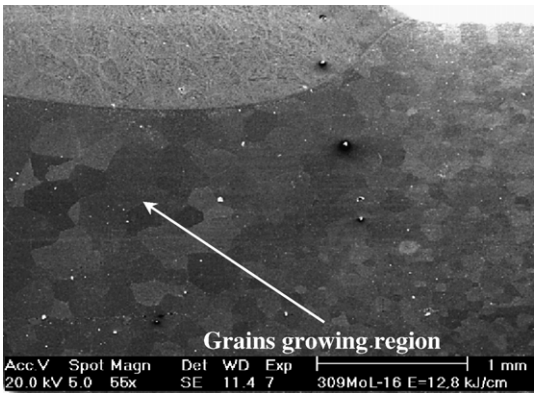

Fig. 4. Scanning electronic microscopy of the transversal section of the sample welded with 8 kJ/cm. It should be noticed the growing of grains situated on the region below the weld bead (55×). Etch: Vilela.

is based on the reaction between the hydrogen sulfide and the surface of the metal, according to Eq. (1).

$$Fe + H_2S \rightarrow FeS + H_2. \quad (I)$$

The result is the formation of iron sulfide as a corrosion product. This product was found on the surface of all the analyzed samples. According to Smith (2003), the main types of sulfide found in corrosive environment contain H_2S. In high temperatures there is the predominance of troilite (FeS), macassite (FeS_2) and also pyrrhotite ($Fe_{1-x}S$) (Craig, 2002). In cases where the concentration of H_2S is very high, there may be the formation of a very complex layer composed of Mackinawite ($Fe_{1+x}S$), troilite (FeS) or pyrrhotite ($Fe_{1-x}S$), covered by a layer of macassite (FeS_2) or pyrite (FeS_2) (Craig, 2002). For this reason, the complete identification of the corrosion products asks for an analysis where more advanced techniques, such as the X-ray diffraction, is used.

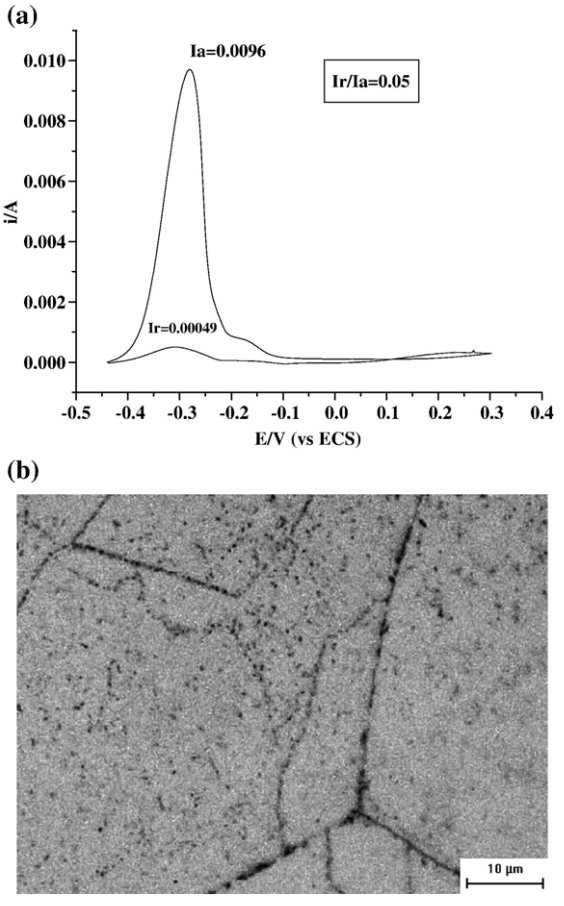

Fig. 5. Sample welded with 6 kJ/cm, without petroleum treatment (a) Polarization curve (b) Micrography of the transversal section (500×). Etch: Vilela.

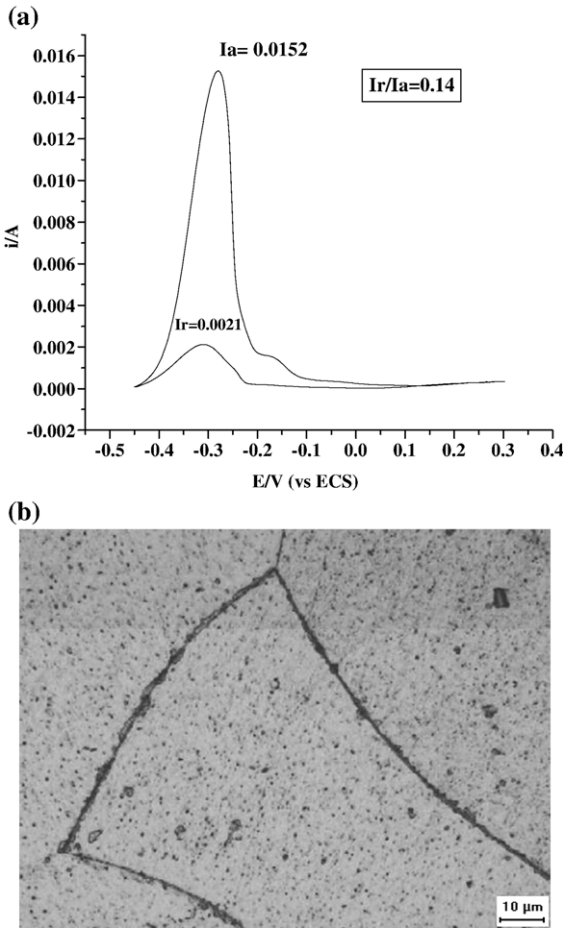

Fig. 6. Sample welded with 8 kJ/cm, without treatment. (a) Polarization curve. (b) Micrography of the transversal section (500×). Etch: Vilela.

3.2. Microstructural analysis

The transversal sections of the samples were analyzed through metallographic exams and considered welded and thermally treated. No significant alterations between the microstructures were observed before and after the treatment. The size of the heat-affected zone grain next to the surface practically did not vary with the increase of the welding energy. This may be due to the non-uniform conduction of heat during the process of welding which, due to the small thickness of the sheet, concentrates the heat in the area below the weld bead, causing the growth of grain in the area right below the welded zone, as shown in Fig. 4.

A more detailed analysis of the enlarged welded specimen revealed the presence of thinly dispersed precipitates in the ferritic matrix and in the grain

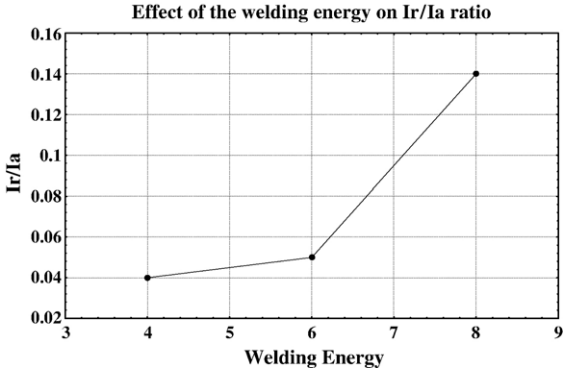

Fig. 7. EPR-DL results for three levels of welding energy.

boundaries (Figs. 5b and 6b). However, its highly reduced dimensions made the identification by SEM and EDX analysis difficult. It may be that the precipitates observed are chromium carbides and/or nitrides derived from the process of welding, since in such areas (adjoining the weld bead) the tried temperatures were above 1000 °C, which, according to the literature (Folkhard, 1988; Silva et al., 2007), favors the precipitation of chromium carbide in ferritic stainless steel.

3.3. Electrochemistry analysis

Through the analysis in the HAZ using the EPR-DL technique, it is possible to observe a small peak in the reverse scanning of the material (Fig. 5a) for the sample welded with 6 kJ/cm, which analysis the passivation layer caused by the anodic scanning, and identifies a perturbation of the passivation layer in this area. These perturbations will initiate the migration of electron from the anodic to the cathodic areas of the material, starting the process of corrosion. The value of I_r/I_a was 0.05, which would characterize a dual structure.

For the sample welded with heat input of 8 kJ/cm, the peak in the reverse scanning was highest and the relation I_r/I_a was 0.14 (Fig. 6a), which indicates a ditch structure. In both cases it would have been expected the presence of some chromium carbide precipitates in the grain boundaries. However, it may be that the mechanism of precipitation of these carbides for the ferritic stainless steel does not occur in the same way as for the austenitic stainless steel.

Although it was not possible to identify the precipitates types in the analysis of the microstructure discussed before. It is believed that those are probably rich in chromium, since the electrochemical analysis detected perturbation in the passivating layer of the steel, which occur exactly because of the chromium depletion in the matrix. Since the temperature of treatment in petroleum immersion to which are submitted the samples is a lot inferior to the temperature of carbide precipitation for the ferritic stainless steel, around 900 °C (Folkhard, 1988; Silva et al., 2007), it is possible to conclude that this increase in the I_r/I_a ratio, and consequently the loss in resistance to corrosion of the material, is due to the levels of welding heat input used in this study. Therefore, the higher the welding heat input, the higher its influence on the perturbation of the passivating layer and the loss of corrosion resistance of the material. Fig. 7 shows the variation of I_r/I_a with the welding heat input.

4. Conclusions

Based on the experimental results on the effect of welding on the corrosion resistance of the heat-affected zone (HAZ) of the AISI 444 ferritic stainless steel in medium containing Venezuelan heavy oil, it was noticed that important metallurgical alterations occurred preferentially in the heat-affected zone (HAZ) by causing a high susceptibility to corrosion. The corrosion product formed on surface was characterized as iron sulfide, indicating that the corrosion process was caused by corrosive substances rich in sulfur, mainly hydrogen sulfide (H_2S). It was also verified that an increasing on the welding heat input leads to an increase in the level of corrosion presented by the material, mainly in high temperatures. Additionally, the temperature of treatment directly influences the start of corrosion, as well as how severe the corrosion process may be. Equally important was the influence of the welding heat cycle that in fact proved to be capable of causing perturbations in the passivation layer, in the steel HAZ adjoining the weld bead. Finally, it is important to noticed that an high concentration of sulfur in the sulfurated compounds favors the formation of extremely aggressive acids, such as the hydrogen sulfide (H_2S), definitely contributing for an accelerated and intense corrosion process of the steel, as it was observed in case studied.

Acknowledgments

Authors thank to the following laboratories: Engesolda-UFC, LACAM / MEV-UFC and Laboratório de Combustíveis e Lubrificantes (LCL-UFC); also to ACESITA and PETROBRAS. CNPq, FINEP and ANP for their support.

References

Cayard, M.S., Kane, R.D., Stevens, C.E., 1994. Evaluation of hydrogen disbanding of stainless steel cladding for high temperature hydrogen service. Corrosion, vol. 94. NACE International, Houston, Texas.

Cortie, M.B., Pollak, H., 1995. Embrittlement and aging at 475 °C in an experimental ferritic stainless steel containing 38 wt% chromium. Mater. Sci. Eng., A Struct. Mater.: Prop. Microstruct. Process. 199, 153–163.

Cosultchi, A., Garciafigueroa, E., Garcia-Borquez, A., Reguera, E., Yee-Madeira, H., 2001. Petroleum solid adherence on tubing surface. Fuel 80, 1963–1968.

Craig, B., 2002. Corrosion products analyses—a road map to corrosion in oil and gas productions. Mater. Perform. 41 (8), 56–58.

Folkhard, E., 1988. Welding Metallurgy of Stainless Steels. Springer-Verlag, New York.

Grobner, P.J., 1973. The 885°F (475 °C) embrittlement ferritic stainless steel. Metall. Trans., A, Phys. Metall. Mater. Sci. 4, 251–260.

Lundin, C.D., Lee, C.H., Menon, R., Stansbury, E.E., 1986. Sensitization of austenitic stainless steels; effects of welding variables on HAZ sensitization of AISI 304 and HAZ behavior of BWR alternative alloys 316 NG and 347. WRC Bull. 319.

Luz, T.S., Farias, J.P., Lima Neto, P., 2006. Use of double loop electrochemical potentiokinetic reaction (DL-EPR) to evaluate the sensitization of austenitic stainless steels after welding. Weld. Int. 20, 959–964.

Machado, J.P.S.E., Silva, C.C., Sobral-Santiago, A.V.C., de Sant'Ana, H.B., Farias, J.P., 2006. Effect of temperature on the level of corrosion caused by heavy petroleum on AISI 304 and AISI 444 stainless steel. Mater. Res. 9 (2), 137–142.

Majidi, A.P., Streicher, M.A., 1986. Four nondestructive eletrochemical tests for detecting sensitization in type 304 and 304L stainless steels. Nucl. Technol. 75 (s/n).

Medvedeva, M.L., 2000. Specifics of high-temperature corrosion processes during oil recovery. Chem. Pet. Eng. 36, 749–754.

Sedricks, A.J., 1996. Corrosion of Stainless Steel. Wiley-Interscience Publications, New York.

Silva, C.C., Ramos Jr., J.M.B., Almeida-Neto, J.C., de Sant'Ana, H.B., Farias, J.P., 2006. Efeito do ciclo térmico de soldagem sobre a resistência à corrosão de aços inoxidáveis empregados como revestimento de torres de destilação de petróleo. Anais do Congresso Latino-Americano de Corrosão, Abraco, Fortaleza. s/n (in portuguese).

Silva, C.C., Farias, J.P., Miranda, H.C., Guimarães, R.F., Menezes, J.W.A., Neto, M.A.M., 2007. Microstructural characterization of the HAZ in AISI 444 ferritic stainless steel. Materials Characterization.

Silva, C.C., Farias, J.P., de Sant'Ana, H.B., submitted for publication. Evaluation of AISI 316L stainless steel welded plates used as lining of petroleum distillation column. Mater. Des.

Smith, S.N., 2003. Corrosion products analysis in oil and gas pipelines. Mater. Perform. 42 (8), 44–47.

Turnbull, A., Griffiths, A., 2003. Corrosion and cracking of weldable 13 wt% Cr martensitic stainless steel for application in the oil and gas industry. Corr. Eng. Sci. Technol. 38 (1), 21–49.